Fischer–Tropsch Synthesis

DOI: 10.1002/anie.201200280

Suppression of Carbon Deposition in the Iron-Catalyzed Production of Lower Olefins from Synthesis Gas**

Ard C. J. Koeken, Hirsa M. Torres Galvis, Thomas Davidian, Matthijs Ruitenbeek, and Krijn P. de Jong**

Utilizing alternative feedstocks to crude oil for the production of olefins is of eminent importance to the chemical industry. Mixtures of carbon monoxide and hydrogen (syngas) produced from natural gas, coal, or biomass can be directly converted into hydrocarbons by the Fischer–Tropsch synthesis (FTS).[1–4] Cobalt- and iron-based catalysts are applied commercially in FTS processes. While cobalt-based catalysts are preferred for the production of long-chain linear alkanes (transportation fuels),[5] iron-based catalysts are attractive for the production of olefins.[2,6–9]

For industrial application of iron catalysts in FTS to produce lower olefins (hereafter designated as Fischer–Tropsch to olefins, FTO) increasing the selectivity to lower olefins (the C_2–C_4 fraction) while suppressing the selectivity to methane remains one of the main challenges.[9] Indeed, the hydrocarbon distribution generally follows the Anderson–Schulz–Flory distribution, which states that at the optimal chain growth probability factor α to obtain the highest proportion of C_2–C_4 olefins (ca. 50 wt %), about 30 wt % CH_4 will also be produced.[7] Generally, methane production can be reduced through increasing α by addition of promoters, such as alkali metals,[10] or lowering the operating temperature.[7]

On the other hand, improving catalyst stability poses an even greater challenge than optimizing selectivity. Several deactivation mechanisms can occur, such as poisoning, sintering, iron phase changes, and carbon deposition.[4,10–12] In particular, at the high temperatures required for FTO, carbon formation by the Boudouard reaction, $2\,CO(g) \rightarrow C(s) + CO_2(g)$, can be significant.[9] If these carbon species are not removed by hydrogenation to hydrocarbons they can block active catalytic sites and eventually cause breakup of catalyst particles when they form carbon filaments.[10,11,13,14] Data on carbon deposition rates obtained under actual FTS conditions are relatively few and are mostly based on ex situ analysis of catalyst samples.[10,15] Obtaining in situ carbon deposition rates under FTS conditions poses a great practical challenge, as the use of a microbalance is usually restricted to atmospheric conditions.[16]

Herein, we describe a method to assess the extent of carbon formation for an iron-based FTO catalyst in situ in combination with online hydrocarbon product analysis. For a novel α-Al_2O_3 supported iron catalyst,[17] we have found conditions where carbon formation was essentially undetectable, while methane production was kept at a low level. Herein, we present the application of the tapered-element oscillating microbalance (TEOM) in FTS research. Previously, the TEOM has been applied for coking studies involving gas-phase reactants and products over heterogeneous catalysts, such as methanol-to-olefins, and the kinetics of carbon nanofiber formation.[18,19] The main advantages of the TEOM over conventional microbalances are the wide range of operating conditions and the plug-flow hydrodynamics,[18] which resemble that of a conventional packed-bed reactor often used in FTS research. This makes a comparison with results from other studies possible and meaningful. In the Supporting Information (section S1) a description of the TEOM setup is given.

The 10 wt % Fe supported on α-Al_2O_3 (10 % Fe/α-Al_2O_3) catalyst was prepared by incipient wetness impregnation with an aqueous solution containing ammonium iron citrate as metal precursor; sodium and sulfur were used as promoters to enhance olefin formation and decrease selectivity to methane, as has been explained previously in more detail.[17] Further details on preparation and characterization are given in the Supporting Information, S2. Prior to FTO conditions, the catalyst was reduced using a 21 vol % H_2 in Ar mixture at 350 °C at 1.7 bar (Supporting Information, S3).

In Figure 1, TEOM results, that is, the mass increase of the catalyst bed with time, are presented for FTO carried out at 20 bar and 350 °C. Time zero indicates the start of the feed of the synthesis gas. From calibration measurements, it is known that from $t = 0$ to $t = 0.2$ h, the mass will change as a result of the replacement of Ar gas by synthesis gas and build-up of carbonaceous species in the catalyst bed. From $t = 0.2$ h to 2 h, mass increase is only caused by buildup of carbonaceous materials in the catalyst bed.At $t \approx 2$ h, the gas feed is switched from synthesis gas to argon again, which caused an increase in the mass as a result of the increase in mass density of the gas flowing through the catalyst bed. There was no significant decrease in mass from $t = 2.3$ to 4 h, which

---

[*] Dr. A. C. J. Koeken, H. M. Torres Galvis, Prof. Dr. K. P. de Jong
Inorganic Chemistry and Catalysis, Department of Chemistry, Utrecht University
Universiteitsweg 99, 3584 CG Utrecht (The Netherlands)
E-mail: k.p.dejong@uu.nl

Dr. T. Davidian, Dr. M. Ruitenbeek
Hydrocarbons R&D, Dow Benelux B.V.
P.O. Box 48, 4530 AA, Terneuzen (The Netherlands)

[**] A.C.J.K. and K.P.d.J. acknowledge support from Dow Benelux. A. van Laak, F. Broersma, and R. van Zwienen are acknowledged for assistance with the oscillating microbalance studies. G. Bonte, A. Chojecki, and C. van Dijk are acknowledged for assistance with the plug-flow reactor experiments. C. van der Spek is acknowledged for the electron microscopy measurements and B. Dickie and K. Scieranka for TGA-MS studies.

Supporting information for this article is available on the WWW under http://dx.doi.org/10.1002/anie.201200280.

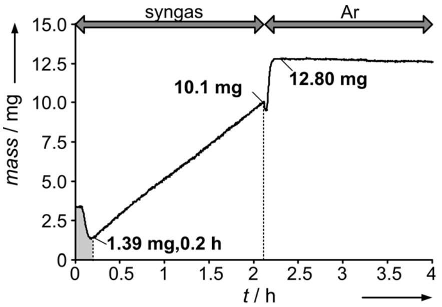

Figure 1. TEOM results showing the mass increase as a function of time on 10%Fe/α-Al_2O_3. Conditions: 20 bar, H_2/CO = 1:1, 350 °C, gas hourly space velocity (GHSV) = 84000 h^{-1}. Mass at $t=0$ h represents the calibrated mass change as a result of replacement of Ar by H_2/CO.

indicated that desorption of FTO products was minimal. Thermogravimetric analysis coupled with mass spectrometry (TGA-MS) on the spent catalyst confirmed that the TEOM measurement was accurate and that mass increase was mainly caused by carbon deposition (Supporting Information, S4). Furthermore, based on engineering criteria accumulation of liquid products in the catalyst bed was not to be expected (Supporting Information, S5).

Evidently, at the conditions presented in Figure 1, severe carbon deposition occurred. The spent catalyst contained 33 wt% carbonaceous material after only about 2 h of FTO. The experiment was terminated after 2 h in order to avoid blockage of the catalyst bed. As a result, the experiment was limited to the initial stage of the FTO reaction. With a weight–time–yield to hydrocarbons (WTY) of $1.1\times 10^{-4}\,\mathrm{mol_{CO}\,g_{cat}^{-1}\,s^{-1}}$ at 2 h, productivity was high (Supporting information, S6). As a result of the duration of this experiment, no conclusions can be drawn regarding the extent of deactivation. The product distribution could be approximated by the ASF distribution. An α value of 0.68 was found (Supporting information, S6).

In Figure 2a, comparison is made between TEM images of the fresh calcined catalyst (a,b) and the spent catalyst (c,d) from the experiment presented in Figure 1. Carbon filaments have formed in large amounts, which explains the relatively fast increase in mass presented in Figure 1.[19] The detachment of a large proportion of the iron particles from the support material as observed here is characteristic of filament formation as well.[13,20] From a comparison of the particle size distributions, it can be concluded that limited sintering has occurred. On the whole, the deposition of carbonaceous materials had a significant effect on catalyst morphology. The extent of carbon formation observed here has to be suppressed to make industrial application of this particular catalyst viable.[10,12]

Despite the extent of carbon formation, a high light-olefin selectivity was obtained with this catalyst (see below). Therefore, we explored the influence of process conditions on the carbon deposition rate, in particular by varying the H_2 and CO partial pressures in the gas feed. Initially, we varied H_2 partial pressure at a fixed CO pressure and vice versa. Both lowering the CO pressure from 10 to 2 bar (at $p_{H_2}=10$ bar) as well as increasing the H_2 pressure form 2.5 to 12.5 bar (at $p_{CO}=2.5$ bar) decreased the rate of carbon deposition. Alternatively, we varied the H_2/CO ratio at total pressures of 2, 10, and 20 bar. Surprisingly, only at a total pressure of 20 bar did we find that at a H_2/CO ratio higher than 4:1, carbon deposition was negligible, as the mass was constant with time within the detection limits of the apparatus. This is illustrated by Figure 3, where the carbon deposition rates and the accompanying WTY, methane selectivities, and C_2–C_4 olefin selectivities as a function of H_2 and CO partial pressure in the gas feed are presented. Comparative data from a conventional fixed-bed plug-flow reactor experiments at standard and high space velocity conditions confirmed the relevance of the TEOM results (Supporting Information, S7). A detailed representation of the catalytic data from two particular experiments, one with negligible carbon deposition and one with significant carbon deposition, is also provided (Supporting Information, S8).

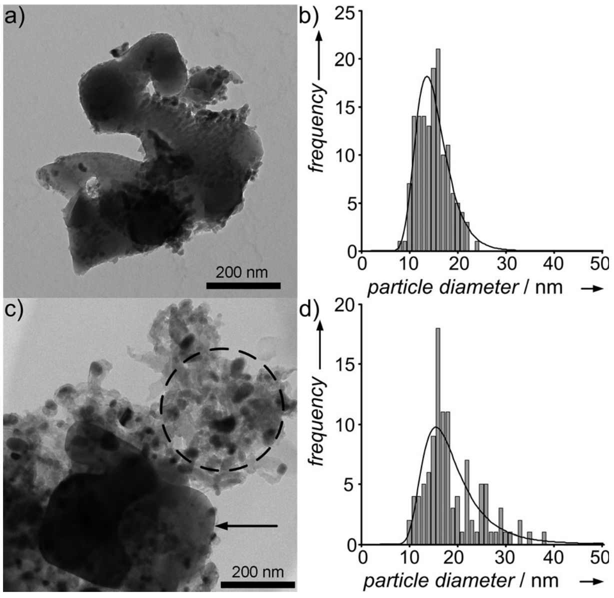

Figure 2. Transmission electron microscopy images and particle size distributions of a), b) fresh and c), d) spent 10%Fe/α-Al_2O_3. The α-Al_2O_3 particles were 200–500 nm in size while the iron particles had average diameter of about 17 nm. The dashed circle in (c) shows a domain with iron particles entangled in carbon filaments, and the arrow indicates an α-Al_2O_3 particle.

Clearly, when opting for a H_2/CO ratio of 1:1, increasing the total pressure resulted in a considerable increase in carbon deposition rate and WTY in combination with a decrease in selectivity for methane and lower olefins (Figure 3). This was in contrast to the case of a H_2/CO of 5:1, where the carbon deposition rate decreased to an undetectable rate when increasing the pressure from about 2 to 20 bar. Moreover, the methane selectivity did not increase substantially with total pressure and remained at a level of 16 wt% at 20 bar. The lower olefin selectivity remained at a high level as well. The highest selectivity for lower olefins was found to be at a low pressure of 2 bar (Figure 3d). However, in that case, the carbon deposition rates were similar to WTY, which was highly undesirable. When increasing the pressure to 20 bar, WTY increased by two orders of magnitude, while carbon

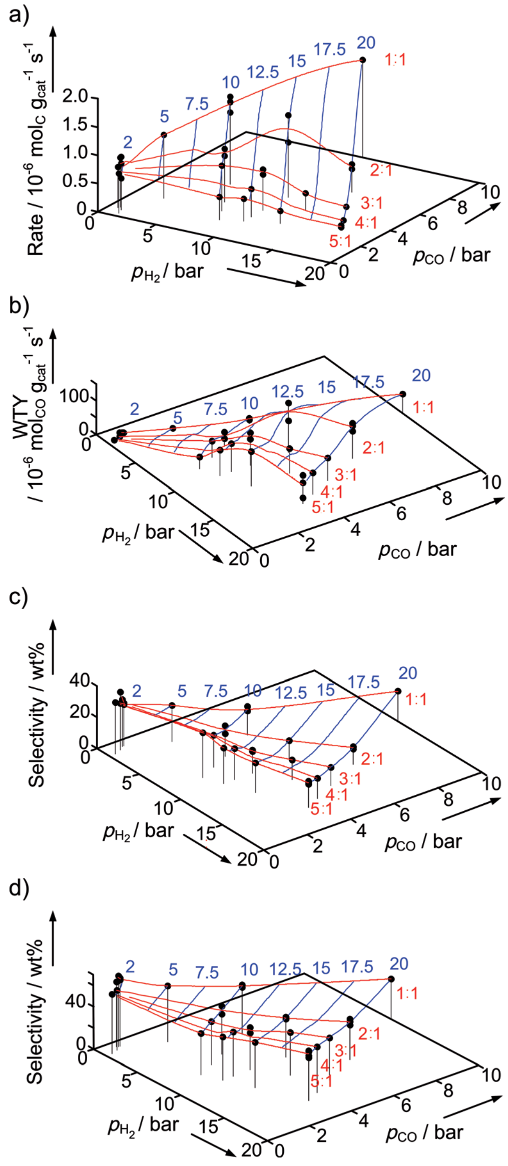

Figure 3. The effect of the partial pressure of H_2 and CO on a) carbon deposition, b) weight-time-yield to hydrocarbon products, c) methane selectivity on CO_2 free basis, and d) C_2–C_4 olefin selectivity on CO_2 free basis. The eight blue lines represent interpolated values of the same total pressure, indicated with blue numbers. The five red lines represent the interpolated values of the same H_2/CO ratio, indicated with red numbers. Conditions: GHSV = 30 000–300 000 h^{-1}, T = 350 °C, time on stream = 4 h.

deposition rates remained of the same order of magnitude. Therefore, for this catalyst formulation, FTO is preferably operated at pressures higher than 10 bar to reach optimal conversions of CO into hydrocarbons.

Most data in Figure 3 were measured at a gas hourly space velocity (GHSV) above 80 000 h^{-1}. These high GHSVs represented more severe conditions for the catalyst than would practically be applied on a commercial scale. Changes in GHSV in the range of 30 000 to 300 000 h^{-1} influenced the carbon deposition rate but not to the extent that the overall trends as given in Figure 3 became significantly different.

Assuming that carbon filament formation is the main mechanism of carbon deposition, several thermodynamic and kinetic factors will play a role.[20,21] Different partial pressures of CO and H_2 will affect the proportions and nature of the iron carbide phases present, which in turn could affect carbon filament growth. Furthermore, nucleation of carbon formation will be affected by Fe particle size, reaction conditions, and the presence of promoters and support.[13] We speculate that at a low total pressure (1–2 bar), even at high H_2/CO ratios, the hydrogen coverage of the iron carbide nanoparticles will be too low to restrict carbon deposition. Only an elevated total pressure (20 bar) in combination with a high H_2/CO ratio will the hydrogen coverage become high enough to minimize carbon formation. Further study is needed to elucidate the role of catalyst morphology and reaction conditions.

In summary, the first application of the TEOM in FTS research has been demonstrated. The TEOM can be applied to obtain in situ information on carbon deposition occurring during high-temperature FTS processes in combination with on-line product analysis. As such the TEOM will be particularly relevant for the development of new iron-based catalysts for the production of chemicals from syngas as an alternative for steam cracking. As a result of this systematic TEOM study, process conditions have been determined where this novel α-Al_2O_3-supported iron catalyst can be applied with a high selectivity to lower olefins, low methane selectivity, and a negligible carbon deposition rate.

Received: January 11, 2012
Revised: April 18, 2012

Keywords: carbon deposition · Fischer–Tropsch synthesis · heterogeneous catalysis · iron · oscillating microbalance

---

[1] J. N. Chheda, G. W. Huber, J. A. Dumesic, *Angew. Chem.* **2007**, *119*, 7298 – 7318; *Angew. Chem. Int. Ed.* **2007**, *46*, 7164 – 7183.
[2] A. Steynberg, *Stud. Surf. Sci. Catal.* **2004**, *152*, 1 – 63.
[3] R. Diercks, J.-D. Arndt, S. Freyer, R. Geier, O. Machhammer, J. Schwartze, M. Volland, *Chem. Eng. Technol.* **2008**, *31*, 631 – 637.
[4] E. de Smit, B. M. Weckhuysen, *Chem. Soc. Rev.* **2008**, *37*, 2758 – 2781.
[5] E. Iglesia, *Appl. Catal. A* **1997**, *161*, 59 – 78.
[6] E. van Steen, M. Claeys, *Chem. Eng. Technol.* **2008**, *31*, 655 – 666.
[7] G. P. van der Laan, A. A. C. M. Beenackers, *Catal. Rev.* **1999**, *41*, 255 – 318.
[8] B. Büssemeier, C. D. Frohning, B. Cornils, *Hydrocarbon Process.* **1976**, *55*, 105 – 112.
[9] Q. Zhang, J. Kang, Y. Wang, *ChemCatChem* **2010**, *2*, 1030 – 1058.
[10] M. E. Dry in *Catalysis—Science and Technology, Vol. 1* (Ed.: J. R. Anderson, M. Boudart), Springer, New York, **1981**, pp. 160 – 255; M. E. Dry, A. Steynberg, *Stud. Surf. Sci. Catal.* **2004**, *152*, 406 – 481.
[11] C. H. Bartholomew, *Appl. Catal. A* **2001**, *212*, 17 – 60.
[12] A. P. Steynberg, R. L. Espinoza, B. Jager, A. C. Vosloo, *Appl. Catal. A* **1999**, *186*, 41 – 54.
[13] K. P. de Jong, J. W. Geus, *Catal. Rev.* **2000**, *42*, 481 – 510.
[14] J. R. Rostrup-Nielsen, J. Sehested, *Adv. Catal.* **2002**, *47*, 65 – 139.

[15] D. J. Moodley, J. van de Loosdrecht, A. M. Saib, M. J. Overett, A. K. Datye, J. W. Niemantsverdriet, *Appl. Catal. A* **2009**, *354*, 102 – 110.

[16] Only known example of a conventional microbalance applied to FTO: A. P. B. Sommen, F. Stoop, K. van der Wiele, *Appl. Catal.* **1985**, *14*, 277 – 288.

[17] H. M. Torres Galvis, J. H. Bitter, C. B. Khare, M. Ruitenbeek, A. Iulian Dugulan, K. P. de Jong, *Science* **2012**, *335*, 835 – 838.

[18] D. Chen, E. Bjorgum, K. O. Christensen, A. Holmen, *Adv. Catal.* **2007**, *51*, 351 – 382, and references therein.

[19] I. Kvande, D. Chen, Z. Yu, M. Rønning, A. Holmen, *J. Catal.* **2008**, *256*, 204 – 214.

[20] A. J. H. M. Kock, P. K. de Bokx, E. Boellaard, W. Klop, J. W. Geus, *J. Catal.* **1985**, *96*, 468 – 480.

[21] For thermodynamic and kinetic aspects related to carbide and carbon formation, see for example: a) E. de Smit, F. Cinquini, A. M. Beale, O. V. Safonova, W. van Beek, P. Sautet, B. M. Weckhuysen, *J. Am. Chem. Soc.* **2010**, *132*, 14928 – 14941; b) I. Alstrup, *J. Catal.* **1988**, *109*, 241 – 251; c) J.-W. Snoeck, G. F. Froment, M. Fowles, *J. Catal.* **1997**, *169*, 240 – 249; d) P. E. Nolan, D. C. Lynch, A. Hall Cutler, *J. Phys. Chem. B* **1998**, *102*, 4165 – 4175.